Supporting Information

Electron Transport via Tyrosine-doped Oligo-Alanine Peptide Junctions: Role of Charges and Hydrogen Bonding

Cunlan Guo,[1,6] Yulian Gavrilov,[2,7] Satyajit Gupta,[1] Tatyana Bendikov,[3] Yaakov Levy,[2] Ayelet Vilan,[4] Israel Pecht,[5] Mordechai Sheves,[1] David Cahen[1]*

Departments of [1]Molecular Chemistry and Materials Science, [2]Chemical and Structural Biology, [3]Chemical Research Support, [4]Chemical & Biological Physics, [5]Immunology, Weizmann Institute of Science, Rehovot, Israel, 761001.

[6]College of Chemistry and Molecular Sciences, Wuhan University, Wuhan 430072, China.

[7]Department of Chemistry, Indian Institute of Technology, Bhilai, India, 492015.

Corresponding Author

*Cunlan Guo, E-mail: cunlanguo@whu.edu.cn.

1. Characterizations of peptide monolayers

Table S1. Structural parameters of the peptide monolayers, calculated from Molecular Dynamic (MD) calculation and measured by ellipsometry.

	Y-1	Y-4	Y-7	7-A
Calculated thickness (Å) *	22.0 ± 0.9	22.3 ± 0.4	24.5 ± 0.5	--
Measured thickness (Å)	15.2 ± 1.7	20.7 ± 1.7	26.7 ± 1.8	19
Measured thickness (after KOH treatment) (Å)	22.8 ± 3.3	30.8 ± 3.7	31.3 ± 6.6	29.9

* Peptide length in the brush is calculated by MD and measured from the S atom of the MPA group to the C terminal residue in the central peptide.

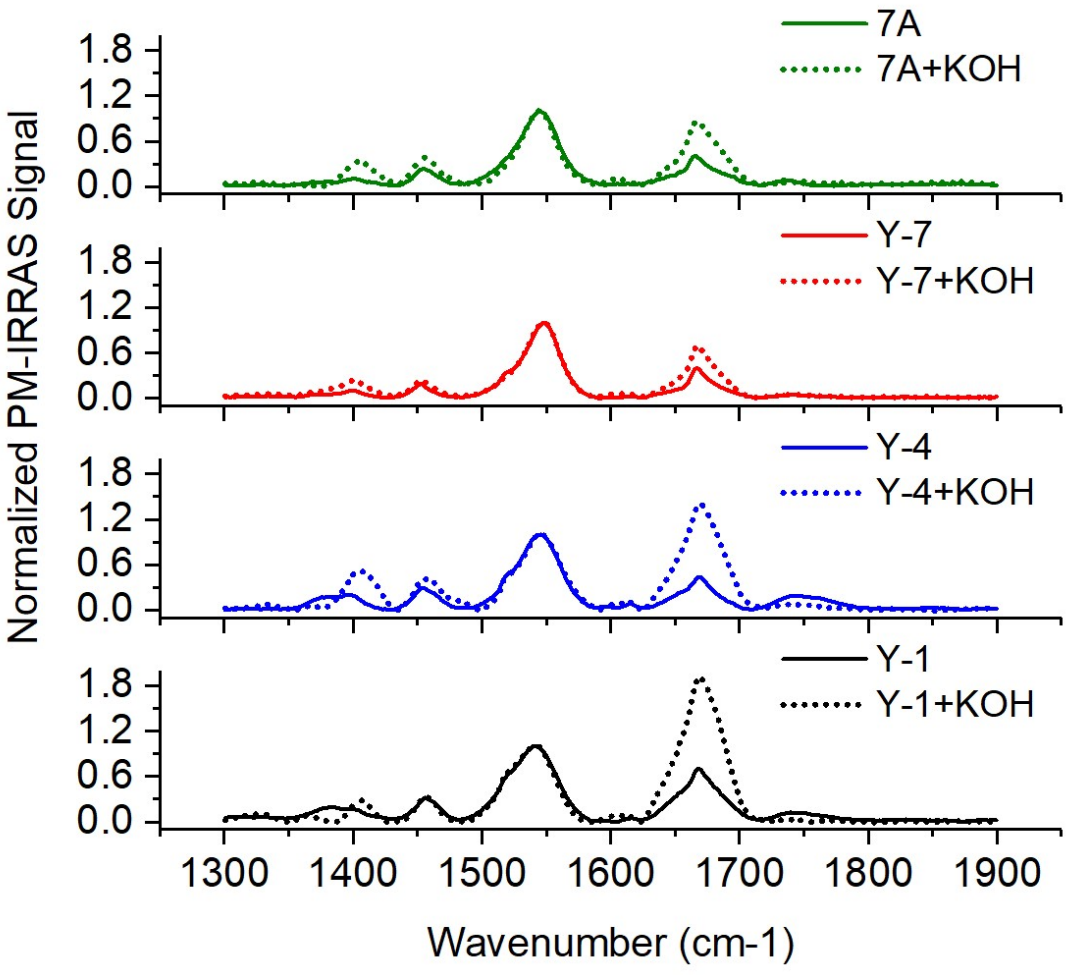

Figure S1. PM-IRRAS of the peptide monolayers before (solid line) and after (dash

line) deprotonation: 7A, Y-7, Y-4, and Y-1 on Au surface. The spectra are normalized by setting amide II peak to 1.

The PM-IRRAS spectra include amide I and II peaks at 1667-1668 and 1541-1548 cm^{-1} for Y-1, Y-4, and Y-7 (Table S2). These peak positions are similar to those observed for 7A. The amide I/II ratio decreases as the Tyr position in the peptide is closer to the C-terminus. The amide I/II ratios of Y-4 and Y-7 are similar to that of 7A, which indicates similarity of peptide orientations in these monolayers. The extra shoulders at 1517 cm^{-1} and small bands at 1597 and 1616 cm^{-1} are observed for all the Tyr-contained peptides, which are assigned to the ν(C=C) of the aromatic ring of the Tyr residue. Especially the disappearance or decrease of the signal at 1517 cm^{-1} indicates the loss of the phenolic hydroxyl proton of Tyr.[1]

Table S2. The amide I and amide II peak positions of the peptide monolayers, obtained from the PM-IRRAS data.

Peptide monolayer	Y-1	Y-4	Y-7	7A	Y-1 +KOH	Y-4 +KOH	Y-7 +KOH	7A +KOH
Amide I (cm^{-1})	1668	1668	1667	1665	1669	1669	1667	1666
Amide II (cm^{-1})	1541	1546	1548	1546	1542	1547	1548	1545
Amide I/II ratio	0.61	0.44	0.40	0.40	1.92	1.41	0.69	0.86

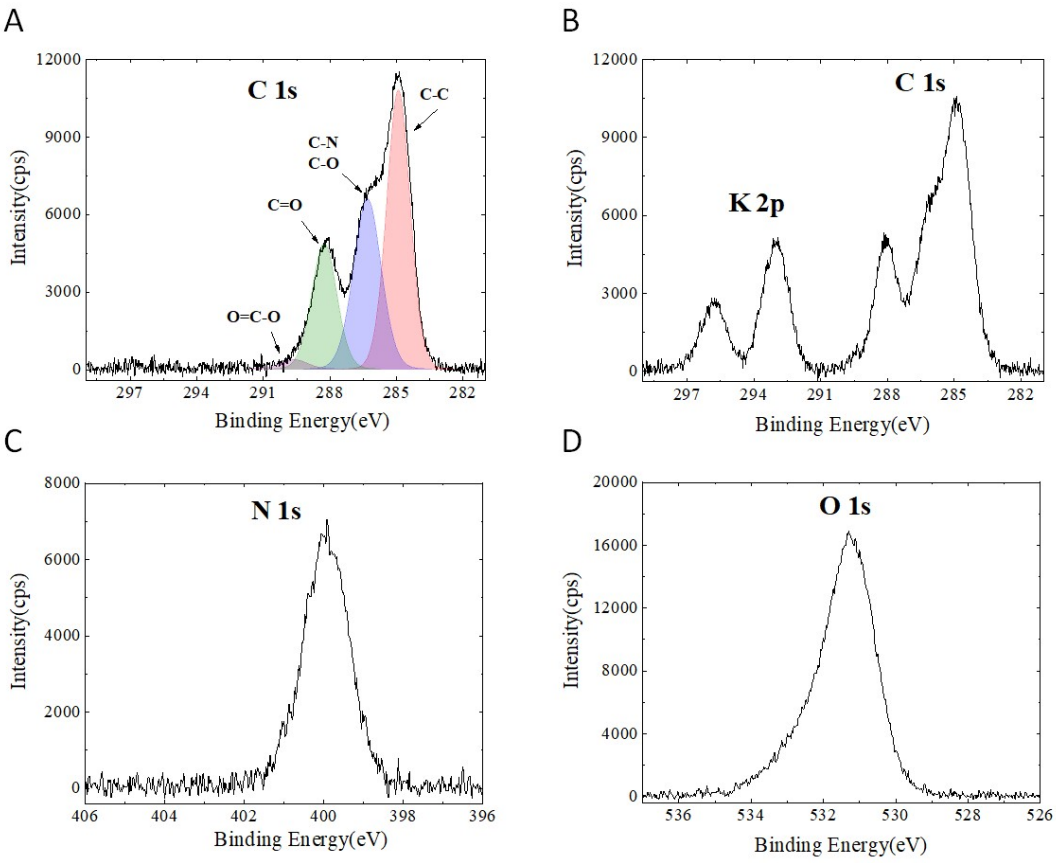

Figure S2. High resolution XPS spectra of Y-7 monolayer as an example. (A) C 1s region of the neutral Y-7 monolayer; (B), (C), and (D) are the C 1s + K 2p, N 1s, and O 1s regions of the deprotonated by KOH Y-7 monolayer on the Au surface.

Table S3. Nitrogen/Potassium and Potassium/Peptide ratios calculated from ARXPS measurements at different tilt angles of Y-1, Y-4, Y-7, and 7A peptide monolayers after KOH treatments.

	Y-1+KOH			Y-4+KOH			Y-7+KOH			7A+KOH		
	0°	45°	65°	0°	45°	65°	0°	45°	65°	0°	45°	65°
N/K	2.41	2.23	2.48	2.27	2.27	2.1	2.6	2.35	2.53	3.32	3.4	3.29
K/peptide	2.9	3.1	2.8	3.1	3.1	3.3	2.7	3.0	2.8	2.1	2.1	2.1

The N/K ratio was calculated from the ARXPS measurements at different tilt angles for all the peptide monolayers. As one peptide molecule ($C_{10}N_7O_{10}S$) contains 7 nitrogen atoms, K/peptide = 7/(N/K ratio).

2. Electron transport measurements

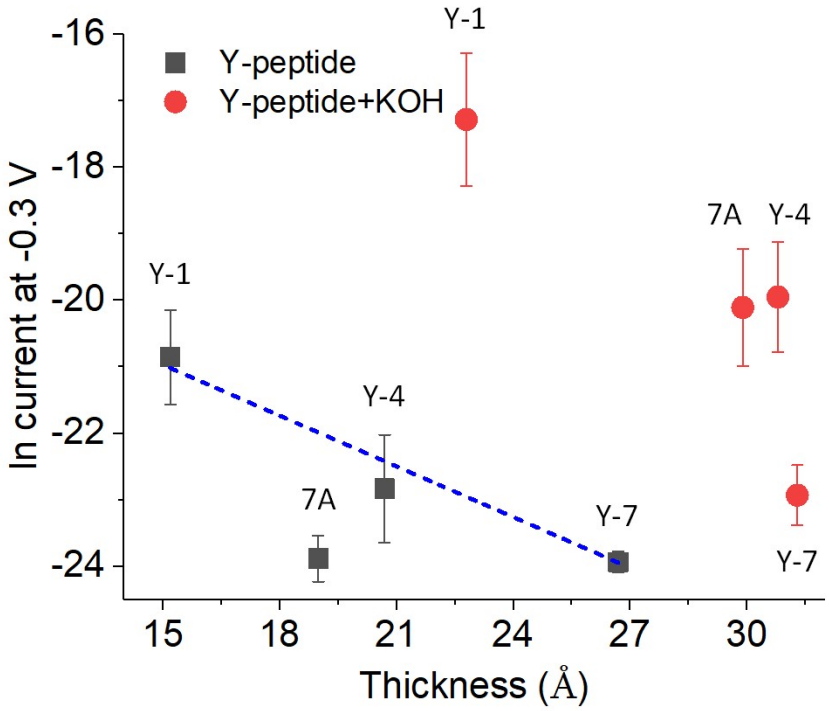

Figure S3. The ln(current) at -0.3 V as the function of peptide monolayer thickness determined by ellipsometry. The black dots from left to right are the peptide monolayers Y-1, 7A, Y-4, and Y-7 under neutral condition. The red dots from left to right are the peptide monolayers Y-1, 7A, Y-4, and Y-7 after alkaline treatment.

Table S4. The comparison of current values recalculated by thickness normalization.

peptide	7A	Y-1	Y-4	Y-7	W-1	W-4	W-7
thickness (Å)	19	15.2	20.7	26.7	21	20	26
thickness ratio to Y-7	0.71	0.57	0.78	1	0.79	0.75	0.97
lnI(exp) at -0.3 V	-23.89	-20.86	-22.84	-23.94	-20.52	-21.04	-19.65
InI(recal) at -0.3 V	-28.51	-27.76	-26.44	-23.94	-23.94	-25.06	-20.07

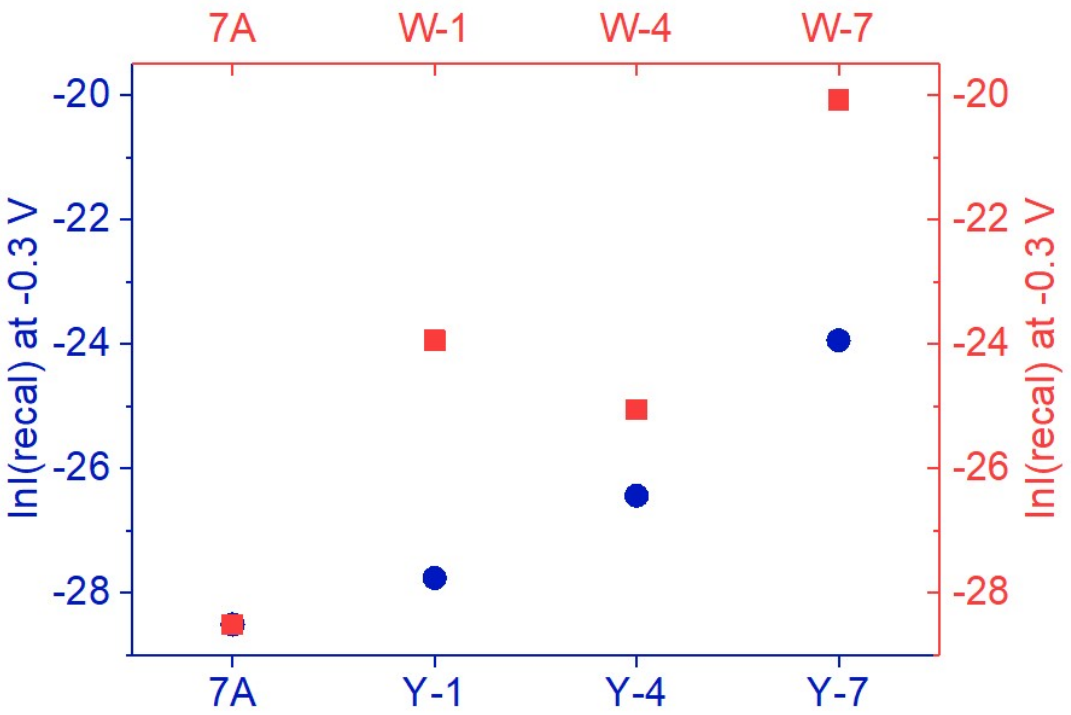

Figure S4. The comparison of recalculated current values by equation 1 for peptide junctions between Y-peptide (blue with left Y-axis) and W-peptide (red with right Y-axis).

To further evaluate the contribution of doped Tyr on peptide electron transport and compare to Trp, we recalculated the current values at a given voltage by normalizing the thickness (l) to the same thickness as Y-7 monolayer and assuming that the natural logarithm of current across peptide junctions follow the linear relationship to thickness with β of 0.6 (Table S4). The current values are recalculated as following.

$$lnI(recal) = lnI(exp) - \beta \times (l(Y\text{-}7) - l(peptide)). \quad (1)$$

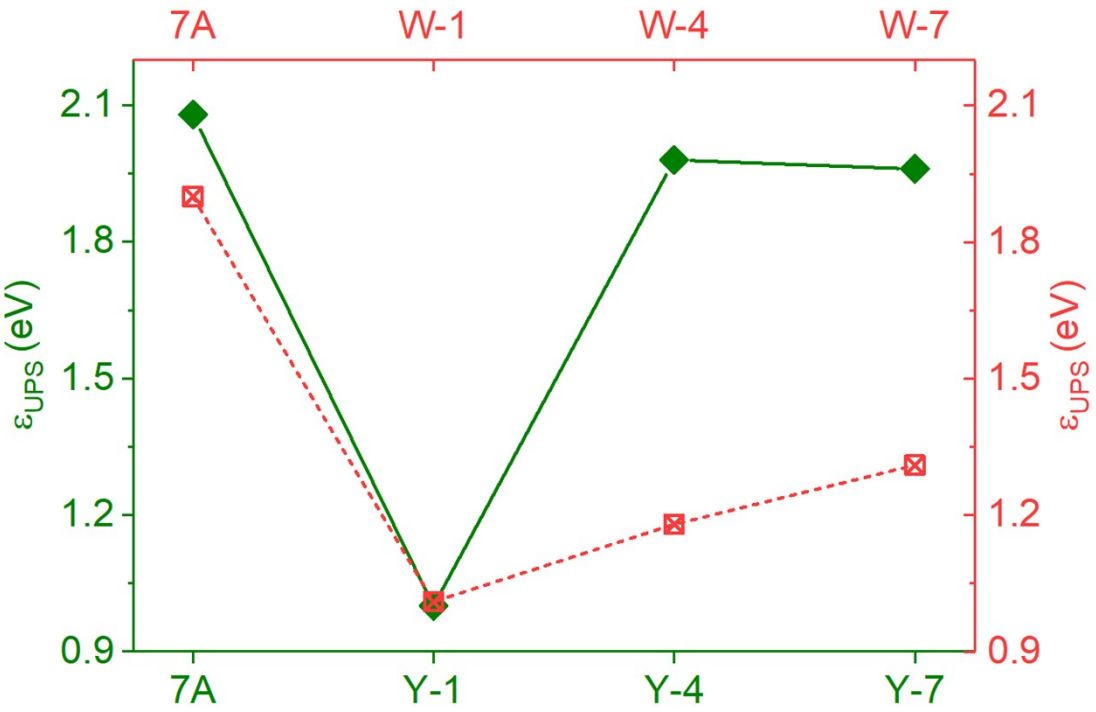

Figure S5. Comparison of UPS-measured energy barriers (ε_{UPS}) between Y-peptides and W-peptides with different Y and W sequences.

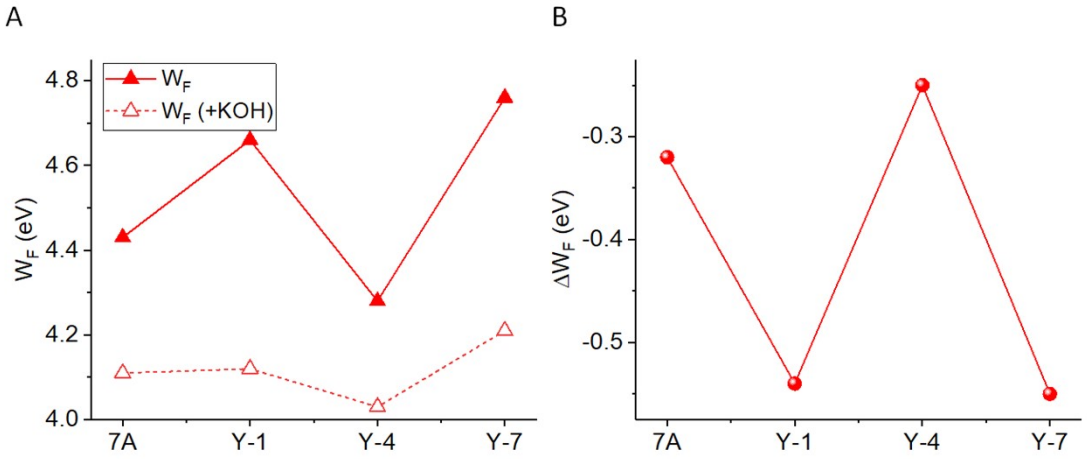

Figure S6. Work function of peptide monolayers on the Au electrode surface: 7A, Y-1, Y-4, and Y-7. (A) The work function of peptide monolayer before (solid triangles) and after alkaline treatment (hollow triangles), (B) The changes of work function upon deprotonation. $\Delta W_F = W_F$ (+KOH) - W_F.

The work functions of the peptide monolayers exhibit fluctuations from 4.15 to 4.8 eV for peptide Y-1 to Y-7 (Figure S6A). The work function values are mainly affected by the Au-S bond. The surface polarization effects[2] or dipole–dipole interactions between peptides[3, 4] which can vary with the Tyr positions in peptide molecules, also contribute to the work function. Upon deprotonation, the work functions decrease to the range of 4.0-4.2 eV, but follow a similar trend as before deprotonation. The changes in work function upon deprotonation, ΔW_F, are scattered (Figure S6B). As angle-resolved X-ray photoelectron spectroscopy (ARXPS) proved that the counter potassium ions are uniformly distributed throughout the peptide monolayer with similar K/peptide ratios (3 for Y-peptides and 2 for 7A), the various W_F value decreases may stem from the extra negative charges forming to neutralize extra potassium ions and the possible peptides dipole moment variations caused by peptides structural alterations following the alkaline treatment.

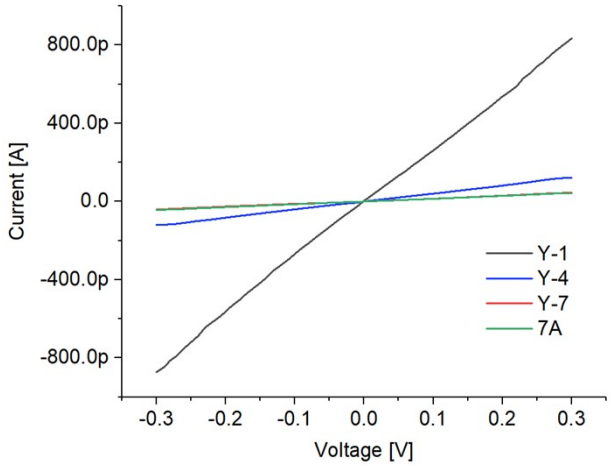

Figure S7. Example of I-V curves in linear format.

3. Molecular Dynamics (MD) simulations

The all-atom MD simulations using the GROMACS package Version 4.5.4[5] and the CHARMM force field[6] were used to study the conformation of the peptide monolayers. A 3 × 3 array with only the sulfur atom fixed in the XY plane was constructed to simulate the monolayer. The simulations were set in vacuum to mimic the dry environment of peptide monolayer.

The equations of motion were integrated using the leap-frog integrator. The systems were minimized with 50000 steps of steepest descent. A cut-off range of 1.0 nm was chosen for the Van der Waals and Coulomb interactions and the Particle Mesh Ewald method[7] was applied to treat long-range electrostatics (4th order cubic interpolation, 0.16 nm grid spacing). The production simulations were run in the NVT ensemble, using velocity rescaling thermostat[8] with the time constant of 1 ps and the reference temperature of 300 K. We applied harmonic constrains to all bonds involving hydrogens using the LINCS algorithm. All the peptides were simulated for 100 ns in order to ensure achieving equilibration.

References

1. A. Barth, *Prog Biophys Mol Bio*, 2000, **74**, 141-173.
2. J. B. Neaton, M. S. Hybertsen and S. G. Louie, *Phys Rev Lett*, 2006, **97**, 216405.
3. G. Heimel, L. Romaner, J. L. Bredas and E. Zojer, *Phys Rev Lett*, 2006, **96**, 196806.
4. F. Rissner, D. A. Egger, A. Natan, T. Koerzdoerfer, S. Kuemmel, L. Kronik and E. Zojer, *J Am Chem Soc*, 2011, **133**, 18634-18645.
5. B. Hess, C. Kutzner, D. van der Spoel and E. Lindahl, *J Chem Theory Comput*, 2008, **4**, 435-447.
6. N. Foloppe and A. D. MacKerell, *J Comput Chem*, 2000, **21**, 86-104.
7. U. Essmann, L. Perera, M. L. Berkowitz, T. Darden, H. Lee and L. G. Pedersen, *J Chem Phys*, 1995, **103**, 8577-8593.
8. G. Bussi, D. Donadio and M. Parrinello, *J Chem Phys*, 2007, **126**, 014101.